

## SCIENTIFIC COMMUNICATIONS

### RECOGNIZING PORPHYRY COPPER POTENTIAL FROM TILL ZIRCON COMPOSITION: A CASE STUDY FROM THE HIGHLAND VALLEY PORPHYRY DISTRICT, SOUTH-CENTRAL BRITISH COLUMBIA

Robert G. Lee,<sup>1,1</sup> Alain Plouffe,<sup>2</sup> Travis Ferbey,<sup>3</sup> Craig J.R. Hart,<sup>1</sup> Pete Hollings,<sup>4</sup> and Sarah A. Gleeson<sup>5,6</sup>

<sup>1</sup>Mineral Deposit Research Unit (MRDU), The University of British Columbia, 2207-2020 Main Mall, Vancouver, British Columbia V6T 1Z4, Canada

<sup>2</sup>Geological Survey of Canada, Natural Resources Canada, Ottawa, Ontario K1A 0E8, Canada

<sup>3</sup>British Columbia Geological Survey, Ministry of Energy and Mines, Victoria, British Columbia V8W 9N3, Canada

<sup>4</sup>Geology Department, Lakehead University, 955 Oliver Road, Thunder Bay, Ontario P7B 5E1, Canada

<sup>5</sup>GFZ Helmholtz Centre Potsdam, Telegrafenberg, 14473 Potsdam, Germany

<sup>6</sup>Institute of Geological Sciences, Freie Universität Berlin, Malteserstrasse, 74-100, Berlin 12249, Germany

#### Abstract

The detrital zircons in tills overlying the Guichon Creek batholith, British Columbia, Canada, have trace element concentrations and ages similar to those of zircons from the bedrock samples from which they are interpreted to have been sourced. Rocks from the core of the batholith that host porphyry copper mineralization have distinct zircon compositions relative to the distal, barren margin. We analyzed 296 zircons separated from 12 subglacial till samples to obtain U-Pb ages and trace element compositions. Laser ablation U-Pb ages of the detrital zircons overlap within error with chemical abrasion-thermal ionization mass spectrometry U-Pb ages of the Late Triassic Guichon Creek batholith and confirm that the detrital zircons are likely derived from the batholith. The youngest intrusions of the batholith produced the Highland Valley Copper porphyry deposits and contain distinctive zircons with elevated  $\text{Eu}/\text{Eu}_N^*$  > 0.4 attributed to high magmatic water contents and oxidation states, indicating higher porphyry copper potential. Zircon from till samples adjacent to and 9 km down-ice from the mineralized centers have mean  $\text{Eu}/\text{Eu}_N^*$  > 0.4, which are indicative of potential porphyry copper mineralization. Detrital zircon grains from more distal up- and down-ice locations (10–15 km) have zircon  $\text{Eu}/\text{Eu}_N^*$  mean values of 0.26 to 0.37, reflecting background values. We conclude that detrital zircon compositions in glacial sediments transported several kilometers can be used to establish the regional potential for porphyry copper mineralization.

#### Introduction

The demand for copper is expected to increase in the next few decades as a result of the growth of developing economies, the electric car revolution, and the requirements for conductors in green technologies (Elshkaki et al., 2016; Ali et al., 2017; Sverdrup et al., 2019). Over the last decade, the average cost per mineral discovery has increased in part due to progressive exploration under cover (Schodde, 2017). Exploration for buried deposits is more challenging and expensive and often less successful (Schodde, 2017); therefore, new tools are required to increase exploration success.

Porphyry copper deposits are a major global source of copper and are formed in magmatic-hydrothermal systems that contain resistate igneous accessory and hydrothermal alteration minerals. The chemistry of accessory minerals such as zircon, apatite, and titanite in magmatic rocks has been used to assess the propensity of an intrusion to generate porphyry copper deposits—a property commonly referred to as porphyry fertility (Ballard et al., 2002; Dilles et al., 2015; Bouzari et al., 2016; Lu et al., 2016, 2019; Lee et al., 2017; Shu et al., 2019). The Ce and Eu—two rare earth elements with dual

valences—compositions of zircon can record the higher oxidation state of fertile magmas compared to barren ones (Ballard et al., 2002; Burnham et al., 2015; Dilles et al., 2015).

Certain minerals from ore systems have chemical compositions reflecting a potential for mineralization. Some of these minerals are resistant to weathering, can be preserved in surficial deposits such as till or stream sediments, and can be used for porphyry exploration under cover (Averill, 2001; Kelley et al., 2011; Plouffe et al., 2016; Plouffe and Ferbey, 2017). Zircon is an ideal indicator due to its robust nature, resistance to secondary alteration, and ability to provide age and compositional records of the magmas from which it crystallized. Although it has been suggested that the composition of zircon grains from detrital sediments could be used in mineral exploration to indicate porphyry mineralization potential in up-ice or river catchment regions (Ballard et al., 2002; Dilles et al., 2015; Lu et al., 2016), the concept has never been fully documented.

In this study, zircon grains were recovered from subglacial till samples acquired at various distances from the ore-forming intrusions and porphyry Cu deposits of the Highland Valley Copper district of south-central British Columbia, Canada. The trace element compositions were acquired from the till

<sup>1</sup>Corresponding author: e-mail, rlee@eoas.ubc.ca

zircon. The objective is to test if the fertility signal recorded in the rare earth element (REE) composition of zircon in the Guichon Creek batholith (Lee et al., 2020) could be detected in detrital grains. Although the composition of detrital zircons from till derived from the nearby Gibraltar porphyry Cu-Mo deposit, Canada, had been addressed (Plouffe et al., 2019), that study had limited samples. Our study is the first to systematically test the variability of a significant number of detrital zircon grains recovered from a suite of regional samples of subglacial till.

### Geology of the Guichon Creek Batholith

The Guichon Creek batholith, British Columbia, Canada, was emplaced into the Late Triassic Quesnel terrane sedimentary and volcanoclastic rocks (McMillan et al., 2009; Byrne et al., 2013; D'Angelo et al., 2017). The N-trending 65- × 35-km batholith comprises at least five concentrically zoned cogenetic magmatic units (Fig. 1). The earliest intrusion within the region is the ~217 Ma Gump Lake stock located along the eastern margin of the batholith (Lee et al., 2020).

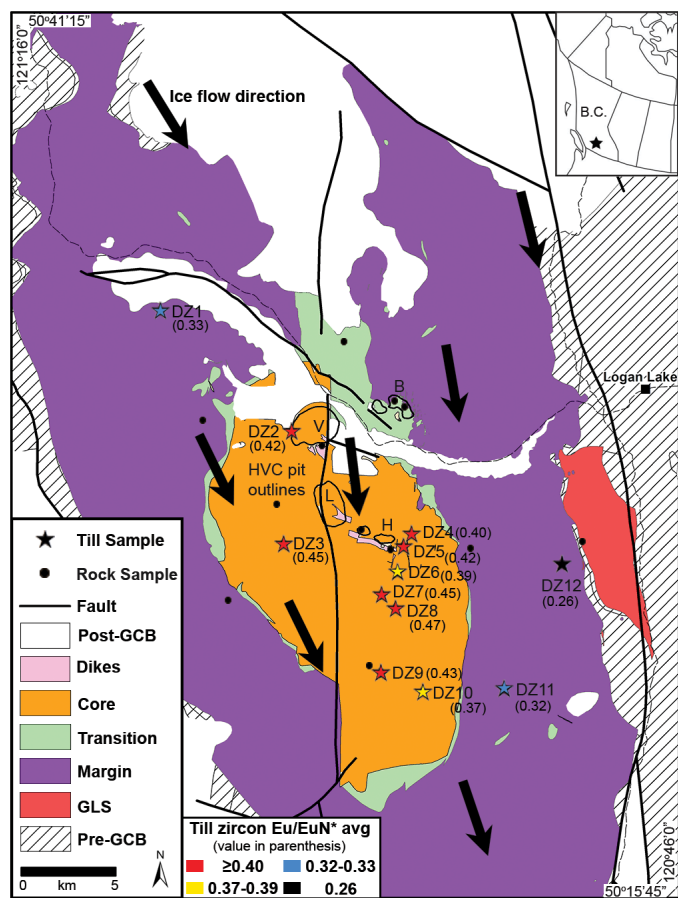


Fig. 1. Simplified bedrock map of the Guichon Creek batholith modified after McMillan et al. (2009). Ice-flow direction and till locations from Ferbey et al. (2016). Average till zircon  $\text{Eu}/\text{EuN}^*$  values determined from this study and highlighted to show distribution from up-ice to down-ice locations. B = Bethlehem deposit, GCB = Guichon Creek batholith, GLS = Gump Lake stock, H = Highmont deposit, L = Lornex deposit, V = Valley deposit. Bedrock sample locations from D'Angelo et al. (2017) and Lee et al. (2020) and represent chemical abrasion-TIMS ages and zircon trace element composition presented in subsequent figures. Inset denotes location of study in south-central British Columbia.

The margin of the batholith consists of gabbros, diorites, and granodiorites, with more felsic granodiorites to monzonites forming the units that constitute the interior and core of the batholith. The age of intrusive rocks ranges from ~218 to ~207 Ma decreasing inward from margin to core (Ash et al., 2006; D'Angelo et al., 2017; Whalen et al., 2017; Lee et al., 2020). The older margin rocks are related to an initial mafic pulse, followed by two to three later evolved magmatic pulses that formed the interior and core (D'Angelo et al., 2017). Multiple centers of porphyry copper-molybdenum mineralization (Fig. 1) are preferentially hosted in the younger phases at or near the core of the batholith (McMillan et al., 2009; Byrne et al., 2013). The porphyry deposits contain over a billion tonnes (Gt) of ~0.25% Cu (Byrne et al., 2013; D'Angelo et al., 2017; Teck Resources Limited, 2019) with the main centers of mineralization forming the Valley, Lornex, and Highmont deposits, which are dated at  $208.4 \pm 0.9$  Ma (Re-Os age; cf. D'Angelo et al., 2017). Additionally, both syn- and post-mineral dikes were emplaced within the core of the batholith, but these units have relatively small volumes compared to the main intrusive phases (McMillan, 1985). Locally, preglacial sediments and volcanic rocks cover these intrusive units (Bobrowsky et al., 1993).

All of the Guichon Creek batholith intrusive units contain zircon as an accessory crystal phase. Trace element composition of zircon from the Guichon Creek batholith records the magmatic evolution of each intrusive unit, and composition of zircon from the younger intrusions correlates with the formation of porphyry copper mineralization (Lee et al., 2020). Due to their size, robust nature, and density, the zircon grains can survive glacial erosion and transport and be recovered from till heavy mineral concentrates.

### Glacial history

The Guichon Creek region is part of the Thompson Plateau, which consists of a gently rolling upland with isolated rounded mountain ridges. Over most of the upland where the tills were sampled, bedrock is mantled by <4 m of till, on average, but up to 10 m in topographically lower areas (Fig. 2a, b; Plouffe and Ferbey, 2015). During the most recent glacial event, termed the Fraser glaciation in British Columbia (Clague and Ward, 2011), which lasted from ca. 28 to 11.5 ka, the southern sector of the Cordilleran ice sheet covered this region and flowed in a south to southeastward direction from an ice divide located to the north, around  $52^\circ\text{N}$  latitude. The orientation of streamlined landforms (flutings, drumlins, crag-and-tails) and striations defines this regional ice movement (Plouffe and Ferbey, 2015). Glacial dispersal of mineralized debris derived from the mineralized zones has resulted in elevated Cu and Mo concentrations (>370 ppm Cu and >5 ppm Mo in the silt plus clay fraction) and high abundances of chalcopyrite (ore mineral; >50 grains/10 kg bulk sediment screened <2 mm) detectable in the till matrix at least 10 km down-ice from mineralized zones (Ferbey et al., 2016; Plouffe et al., 2016; Plouffe and Ferbey, 2017). These dispersal patterns confirm that copper and molybdenum mineralization at Highland Valley Copper was exposed to glacial erosion. However, some of the mineralization is overlain by Eocene volcanic rocks and preglacial sediments, resulting in limited glacial erosion of

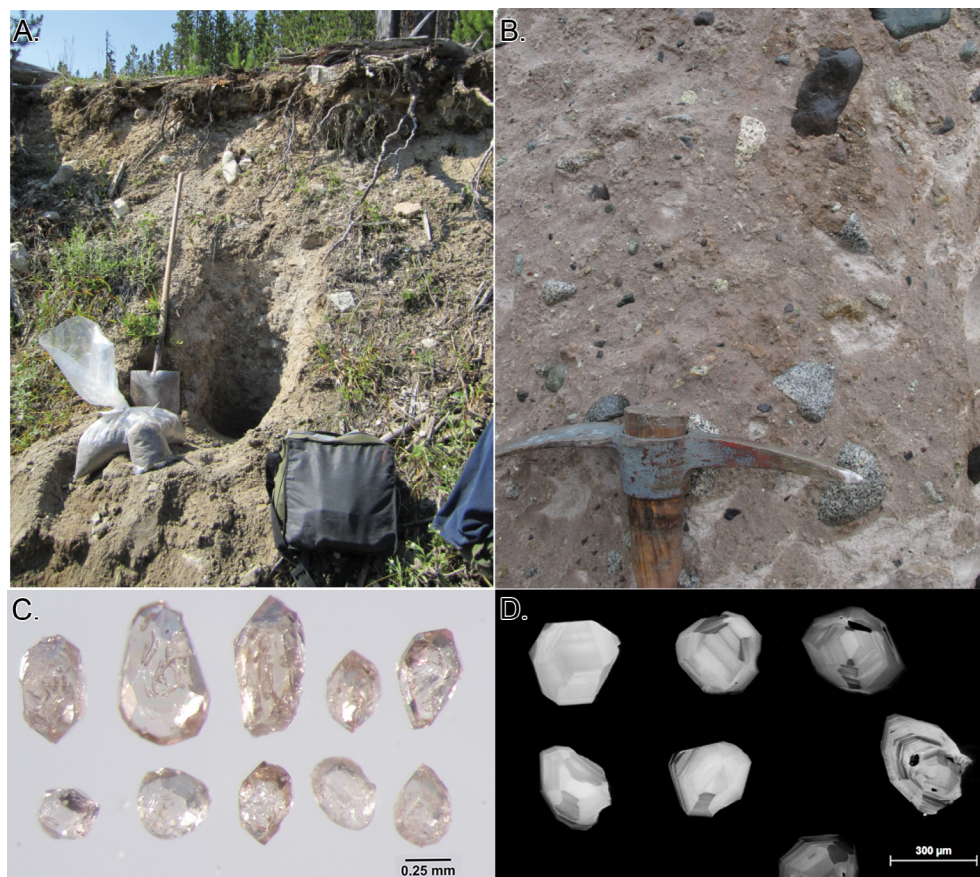


Fig. 2. A. Typical till sampling site in a roadside section. Shovel for scale is 155 cm. B. Massive diamicton with pebble- to cobble-sized clasts in a silty-sand matrix interpreted as subglacial till. The pick-hoe is 46 cm long. C. Selected images of zircon recovered from till in the Guichon Creek batholith region. D. Selected representative cathodoluminescent images of till zircon grains. The majority of the grains were rounded or broken with distinct oscillatory growth zoning and sector zoning.

the syn- to postmineral dikes in this area (Bobrowsky et al., 1993; D'Angelo et al., 2017; Reman, 2019).

## Methods

### *Till sampling strategy*

Twelve till samples were collected within the Guichon Creek batholith region at depths of 130 to 150 cm below the surface in well-compacted, massive, generally fissile, silty-sand to sandy-silt diamictons with abundant striated clasts (Fig. 1; Ferbey et al., 2016). These deposits are interpreted as a subglacial till facies (Fig. 2a, b). Nine to 15 kg of till were processed to recover a heavy mineral concentrate (0.25–0.5 mm; >3.2 specific gravity) as outlined in Ferbey et al. (2016). The majority of the samples were selected from within the core of the batholith at distances of 0.25 to 10 km down-ice from mineralization (Fig. 1). Sample DZ 1, located 10 km up-ice from the main deposits at Highland Valley, and DZ 11, located 12 km down-ice from the main mineralization, occur within the marginal rocks of the batholith (Table 1). Sample DZ 12 is also within the margin of the Guichon Creek batholith but sits off-trend of the glacial transport direction of mineralization and the fertile magmatic rocks.

Zircon grains ( $n = 296$ ) were picked from the heavy mineral concentrates of the 12 selected till samples (Fig. 2c).

Fourteen to 31 zircon grains per sample were put into grain mounts and evaluated under transmitted and reflected light and cathodoluminescence images (Fig. 2d) collected using a Philips XL-30 scanning electron microscope (SEM). Uranium-Th-Pb age dating and trace element composition were determined by laser ablation-inductively coupled plasma-mass spectrometry (LA-ICP-MS) at the Pacific Center for Isotopic and Geochemical Research (PCIGR) at the University of British Columbia, with at least two analytical spots per grain using the methodology described in Lee et al. (2020). A detailed description of till sampling methods, processing, and analytical protocols is provided in Appendix 1, "Sampling Methods and Analytical Techniques," with full results provided in Appendix Table A1.

### *Mineralization proxy*

Zircons do not directly indicate mineralization in magmatic rocks, but their trace element compositions can be used to characterize the magmatic conditions and compositions at the time they crystallized. In oxidized hydrous magmas that form porphyry copper deposits, zircons are characterized by weaker negative Eu anomalies ( $\text{Eu}/\text{Eu}_N^*$ ), which are typical of arc melts because of the suppression of plagioclase fractionation due to high water content, and thus less Eu uptake in the mineral and its enrichment in the residual melt (Ballard et al.,

Table 1. Guichon Creek Batholith Till Sample List with Zircon Ce and Eu Anomaly Values

Sample	Distance to HVC <sup>1</sup> (km)	Longitude	Latitude	Ice Flow	Grains <sup>2</sup>	Spots <sup>3</sup>	Eu/Eu <sub>N</sub> <sup>*</sup> value <sup>4</sup>		Ce/Ce <sub>C</sub> <sup>*</sup> value <sup>5</sup>	
							Range	Avg.	Range	Avg.
DZ1	10; V	-121.159	50.543	Up-ice	31	60	0.19–0.63	0.33	42–2,612	634
DZ2	0.25; V	-121.064	50.485	Lateral up-ice	30	59	0.22–0.82	0.42	53–9,225	795
DZ3	6.5; V	-121.073	50.432	Lateral down-ice	14	21	0.22–0.83	0.45	72–5,208	858
DZ4	1.0; H	-120.976	50.434	Lateral down-ice	28	44	0.18–0.74	0.40	44–8,944	1,025
DZ5	0.5; H	-120.984	50.429	Down-ice	20	35	0.18–0.72	0.42	53–4,822	743
DZ6	1.5; H	-120.987	50.417	Down-ice	15	28	0.21–0.79	0.39	57–1,253	451
DZ7	6.0; L	-120.999	50.405	Down-ice	30	52	0.19–0.76	0.45	93–1,814	683
DZ8	6.25; L	-120.991	50.399	Down-ice	27	46	0.24–0.78	0.47	43–9,730	1,030
DZ9	9.0; L	-121.001	50.368	Down-ice	22	38	0.25–0.70	0.43	63–2,957	675
DZ10	10; L	-120.971	50.359	Down-ice	18	35	0.15–0.89	0.37	43–4,326	962
DZ11	12; L	-120.912	50.36	Down-ice	30	60	0.18–0.61	0.32	47–3,118	832
DZ12	9.0; H	-120.866	50.417	Lateral down-ice	31	59	0.13–0.36	0.26	54–4,045	871

<sup>1</sup>Direct line distance from Highland Valley Copper (HVC) porphyry deposit; H = Highmont, L = Lornex, V = Valley

<sup>2</sup>Total number of grains recovered and picked for analysis by LA-ICP-MS

<sup>3</sup>Number of analytical spots used per sample after quality control validation of data set

<sup>4</sup>Europium anomaly calculated after Dilles et al. (2015)

<sup>5</sup>Cerium anomaly calculated after Lee et al. (2020)

2002; Burnham et al., 2015; Dilles et al., 2015; Lu et al., 2016, 2019; Lee et al., 2017). Europium in magmatic zircon can be used as an indicator of the magmatic oxidation state, high water content, and coincident release of SO<sub>2</sub>-rich magmatic-hydrothermal ore fluid (Dilles et al., 2015); therefore, Eu/Eu<sub>N</sub><sup>\*</sup> is an indicator for porphyry copper mineralization potential.

Similar to Eu/Eu<sub>N</sub><sup>\*</sup>, the Ce<sup>+4</sup>/Ce<sup>+3</sup> ratio in zircon is a proxy for magmatic oxidation state and, therefore, an indicator of an intrusion potential to form porphyry mineralization (Ballard et al., 2002). However, the calculation of the Ce<sup>+4</sup>/Ce<sup>+3</sup> ratio in zircon requires whole-rock geochemical composition and assumptions about the nature of the partitioning of REEs between zircon and melt (Ballard et al., 2002). Since detrital zircon grains are detached from their host rock, their whole-rock composition cannot be determined and used to calculate the Ce<sup>+4</sup>/Ce<sup>+3</sup> ratio. To overcome this limiting factor, we use the Ce/Ce<sub>C</sub><sup>\*</sup> ratio, which is calculated using a power equation curve of the zircon middle and heavy rare earth elements (MREEs and HREEs) to determine Ce<sup>\*</sup>, as a proxy to magma redox conditions (Zhong et al., 2019; Lee et al., 2020). Additionally, we evaluate the Ce/Nd ratio and Y concentrations in zircon, as they have also been shown to identify fertility potential (Lu et al., 2016). The zircon magmatic oxybarometer equation of Loucks et al. (2020) was used to determine change in the fayalite-magnetite-quartz redox buffer ( $\Delta$ FMQ) in the detrital samples. All results and  $\Delta$ FMQ calculation are presented in Appendix Table A1.

### Results: Till Zircon Age and Composition

Uranium-Th-Pb ages and trace element concentrations were determined from 564 spot analyses on 296 till zircons grains. Detrital zircon ages have a Gaussian distribution and range from 240 to 190 Ma, with the highest frequencies correlating with the accepted age range of the batholith 218 to 207 Ma (Fig. 3; D'Angelo et al., 2017; Lee et al., 2020). Ninety-nine percent of the analyses are Late Triassic in age with one grain yielding an Eocene age (App. Table A1). This Eocene zircon is not considered in the following reported results.

Hafnium concentrations in the detrital zircon range from 8,000 to 14,500 ppm (Fig. 4), and trace element concentrations vary in the following ranges: Y (149–1,814 ppm), Nb (0.09–1.25 ppm), Ta (0.046–1.148 ppm),  $\Sigma$ REE (138–1,329 ppm), Th (3.9–305 ppm), and U (22–774 ppm). Values of Nb, Ta, Th, and U positively correlate with Hf in the detrital zircon (Fig. 4). These ranges of concentrations are characteristic of granitic zircons in general (Belousova et al., 2002) and the Guichon Creek batholith specifically (Lee et al., 2020).

Eu/Eu<sub>N</sub><sup>\*</sup> values in till zircons vary within each sample and range from 0.13 to 0.89 (Fig. 5). Following a northwest-southeast transect parallel to ice-flow movement, the average Eu/Eu<sub>N</sub><sup>\*</sup> values fluctuate from 0.3 in up-ice sample DZ1,

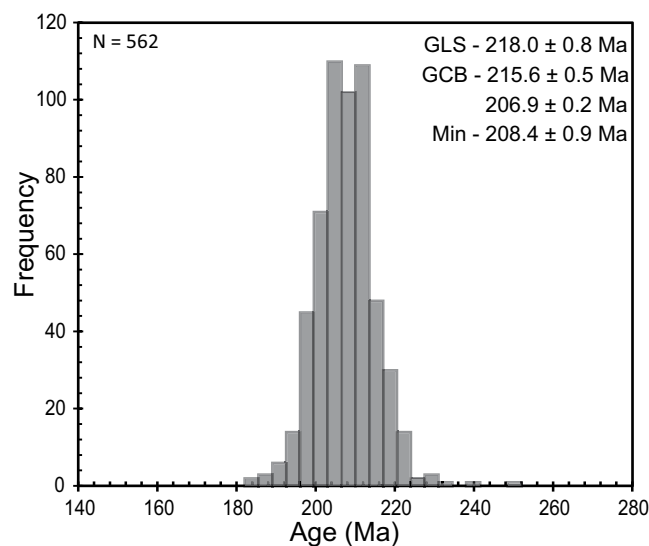


Fig. 3. Histogram of U/Pb LA-ICP-MS ages for detrital zircon grains, bin width approximately  $2\sigma$ . Ages listed in diagram represent chemical abrasion-TIMS and SHRIMP-RG bedrock ages. GCB = U-Pb age distribution of Guichon Creek batholith rocks (D'Angelo et al., 2017; Whalen et al., 2017), GLS = Gump Lake stock (Lee et al., 2020), Min = age of mineralization at Lornex deposit (Re-Os, cf. D'Angelo et al., 2017).

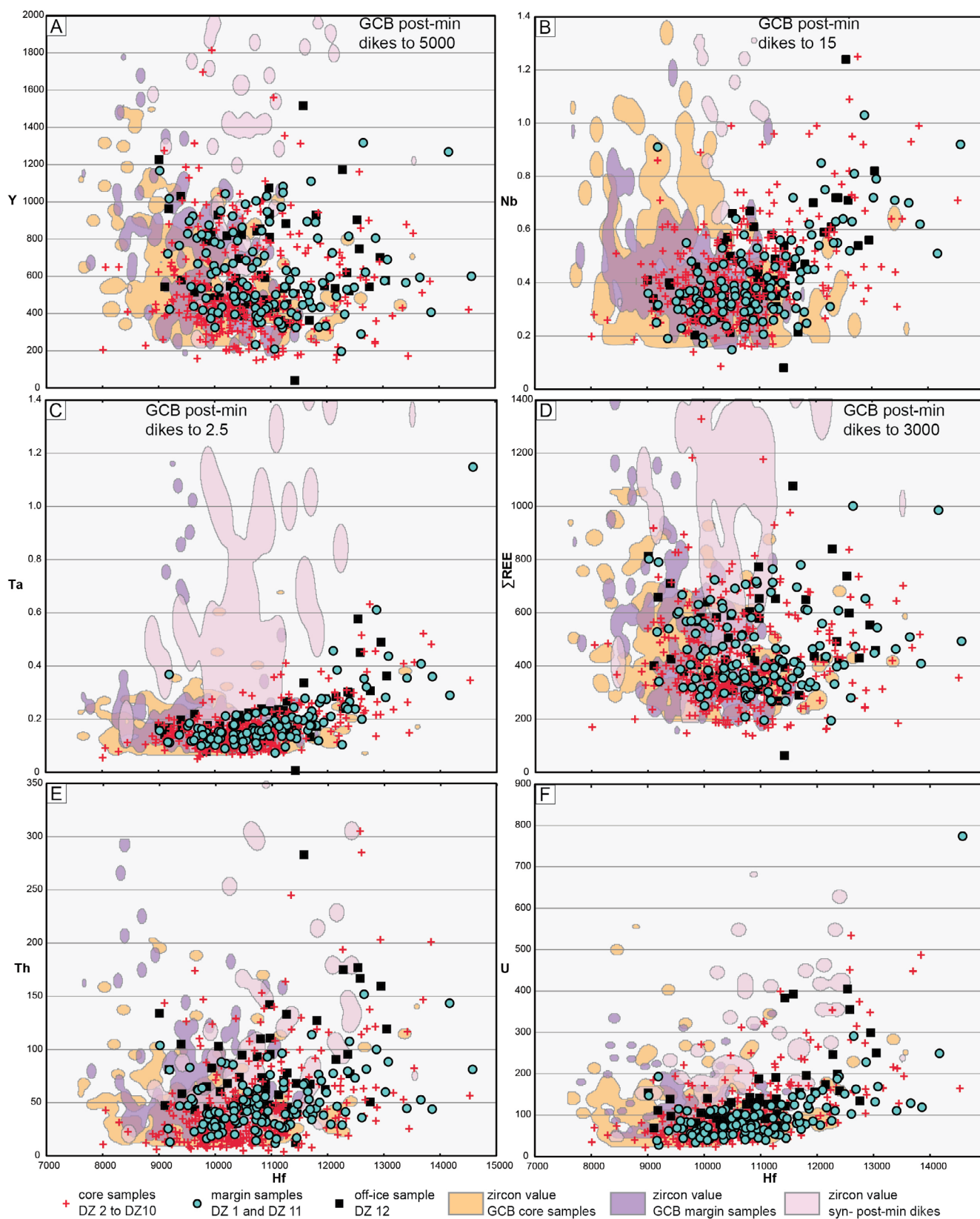


Fig. 4. Plots of Guichon Creek (GCB) batholith detrital zircon hafnium composition versus A. Y, B. Nb, C. Ta, D.  $\Sigma$ REE, E. Th, and F. U. All data listed in ppm; see Appendix Table A1 for concentration of all REE values. Shaded fields represent the range of concentrations observed in samples from Guichon Creek batholith margin, core and syn- to postmineralization dikes from Lee et al. (2020).

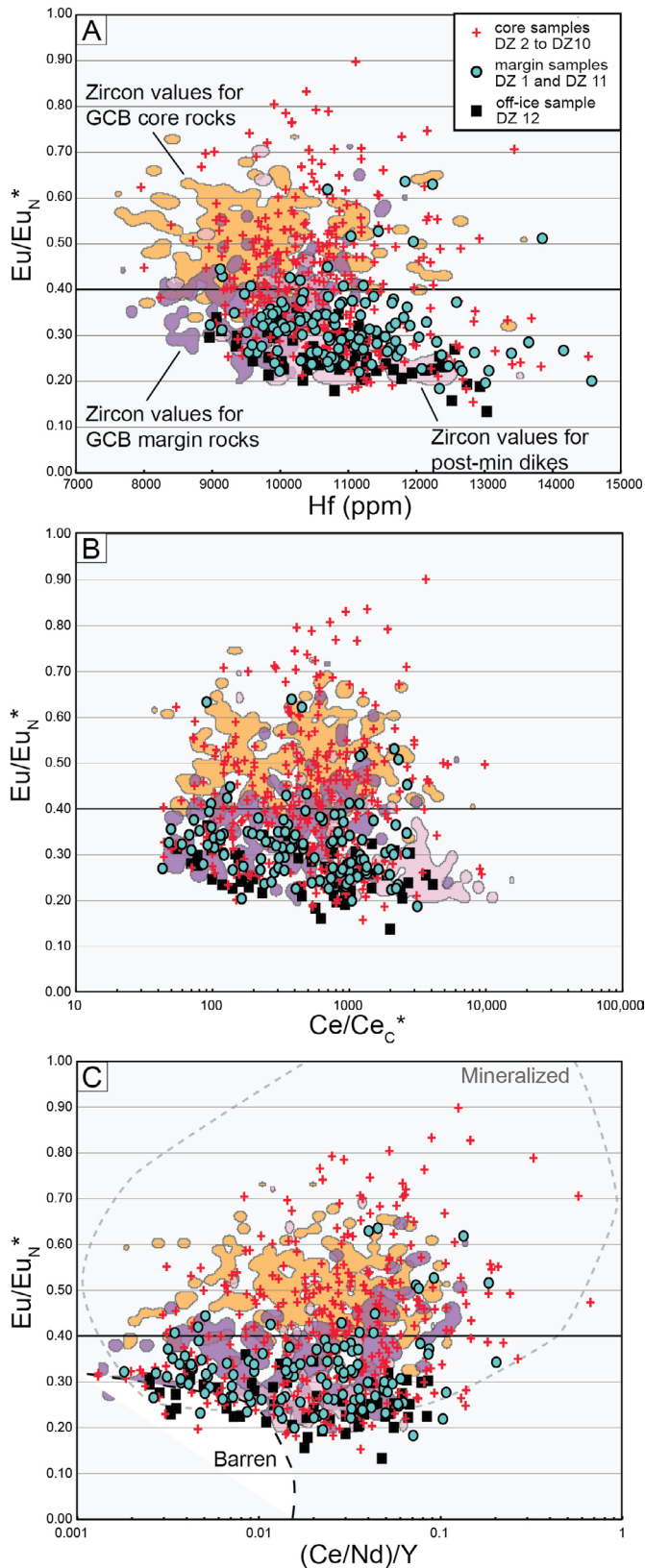


Fig. 5. Plots of detrital zircon composition. A. Hf versus  $\text{Eu}/\text{Eu}_N^*$  (modified after Lee et al., 2020). B.  $\text{Eu}/\text{Eu}_N^*$  versus  $\text{Ce}/\text{Ce}_C^*$ . C.  $(\text{Ce}/\text{Nd})/\text{Y}$  versus  $\text{Eu}/\text{Eu}_N^*$  (barren/mineralized boundary modified after Lu et al., 2016). Value of 0.4 for  $\text{Eu}/\text{Eu}_N^*$  used to define approximate fertile and barren regions after Ballard et al. (2002).

remain  $\geq 0.4$  for over 9 km down-ice from mineralization in seven samples out of eight (DZ2 to DZ9), and are  $< 0.4$  further down-ice (Fig. 6a; Table 1). Zircons from the sample above the marginal zone of the intrusion (DZ12) yielded an average  $\text{Eu}/\text{Eu}_N^*$  value of 0.26 (Fig. 6a). Over 56% of the  $\text{Eu}/\text{Eu}_N^*$  values for samples DZ2 to DZ9 (samples down-ice from mineralization) are  $\geq 0.4$ , compared to 13% of the values for samples DZ1, DZ10, and DZ11 (up-ice and distal down-ice flow).

The  $\text{Ce}/\text{Ce}_C^*$  values in till zircon, calculated using the methods described in Lee et al. (2020), range from 42 to 9,730 (Table 1; Fig. 5B). Along the northwest-southeast transect, the higher average  $\text{Ce}/\text{Ce}_C^*$  values are centered on the core of the intrusion, but there is no clear systematic pattern with increasing distance down-ice (Fig. 7; Table 1). The highest  $\text{Ce}/\text{Ce}_C^*$  ratios in till ( $> 8,000$ ) occur in zircons from samples DZ2, DZ4, and DZ8 that are located directly adjacent to mineralization and 6 km down-ice from mineralization.

Lastly, we applied Loucks et al. (2020) magmatic oxybarometer using the Ti, Ce, and U content of zircon. Calculated  $\Delta\text{FMQ}$  values after Loucks et al. (2020), range from  $-2.75$  to  $2.39$  in till zircon grains. The average and mean values are similar across all 12 till samples with no difference between samples located up-ice and down-ice from the mineralized core or from the marginal zone. In the Guichon Creek batholith samples from Lee et al. (2020), the calculated  $\Delta\text{FMQ}$  values range from  $-1.5$  to  $4.5$ , with the highest values occurring in the syn- to postmineral dikes located in the core of the batholith. Box and whisker plots of zircon  $\Delta\text{FMQ}$  in the various phases of the Guichon Creek batholith and in till along the northwest-southeast transect are provided in Appendix Figure A1.

## Discussion

The ages of the till zircon grains are consistent with an origin from the Guichon Creek batholith, as would be expected from samples collected in subglacial till overlying the intrusion (Fig. 3). Till zircon ages are within error of the accepted age range of the Guichon Creek batholith (Fig. 3), using the LA-ICP-MS analytical method, which has larger uncertainties than the single-crystal thermal ionization mass spectrometry (TIMS) or SHRIMP-RG determinations used by D'Angelo et al. (2017), Whalen et al. (2017), and Lee et al. (2020). A Guichon Creek batholith provenance for most till zircon grains is also indicated by their trace element compositions (Y, Nb, Ta, Th, U, REEs); these match published values (Fig. 4; Lee et al., 2020). The compositions of some till zircon grains do not correspond to the Guichon Creek batholith composition fields defined by Lee et al. (2020) (Fig. 4). These uncorrelated till grains could have originated from unknown lithological sources, both distal to and within the Guichon Creek batholith, that were not sampled by the Lee et al. (2020) study. Given that ages of the till zircons correspond to the Guichon Creek batholith, we interpret the population of zircon grains in till to be dominantly derived from the underlying Guichon Creek batholith with potentially rare grains from unknown sources. Therefore, we did not reject any zircon grains from our composition study. Lastly, based on composition alone, the till zircon grains are unlikely to be derived from younger dikes, which have distinct zircon composition compared to the main Guichon Creek batholith intrusions and till zircon

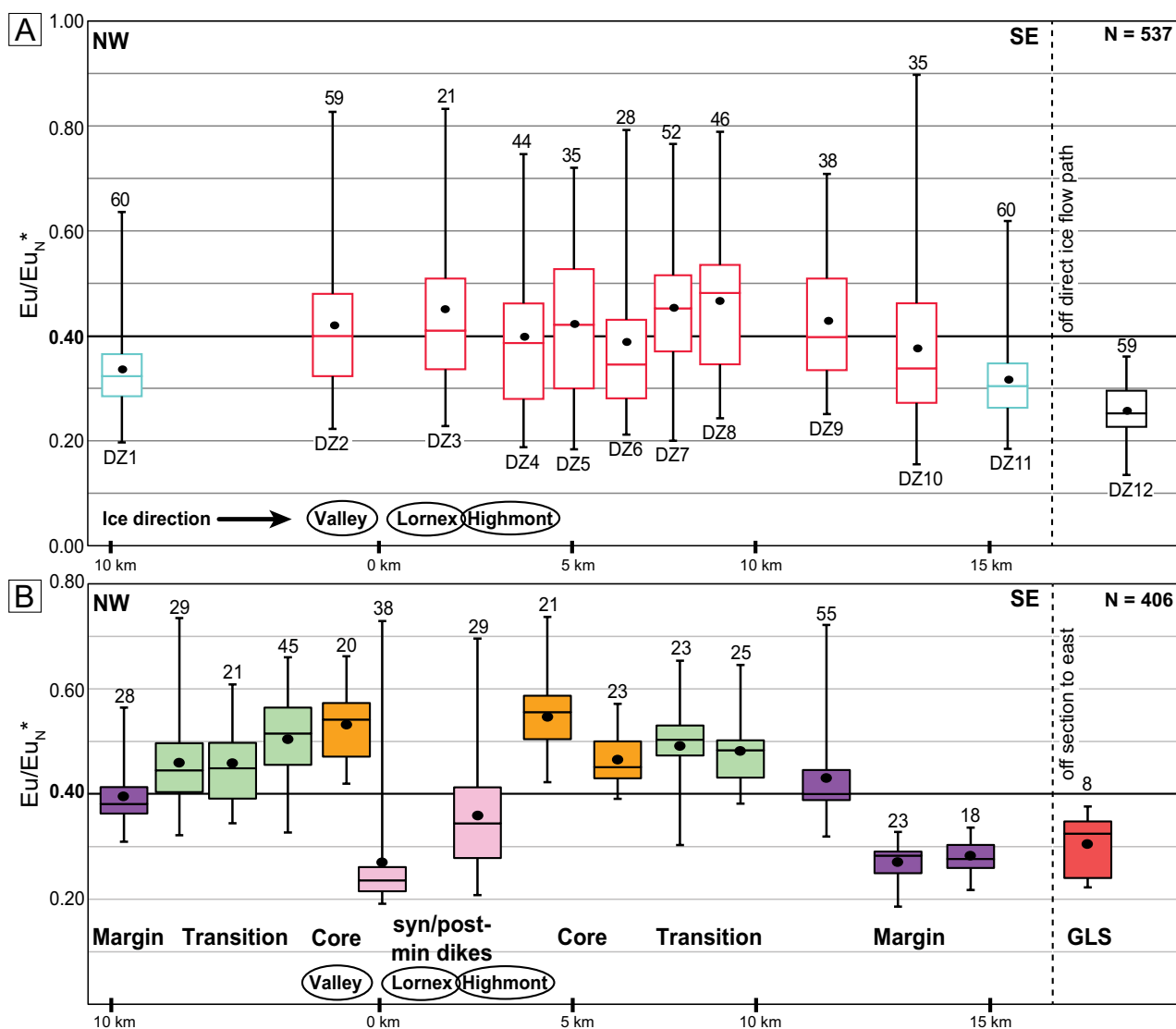


Fig. 6. Box and whisker plots of  $\text{Eu}/\text{Eu}_N^*$  zircon composition for A. detrital zircon grains presented approximately along northwest-southeast section with distance up- and down-ice from Highland Valley Copper deposits (see Fig. 1) and B. Guichon Creek batholith rocks after Lee et al. (2020). Shaded color distribution fields of bedrock samples correlate with Figure 1; colored boxes in detrital samples correlate with Figure 3. Detrital samples adjacent to and down-ice from bedrock core samples that host mineralization have elevated  $\text{Eu}/\text{Eu}_N^*$  values, whereas samples up-ice and along margin have  $\text{Eu}/\text{Eu}_N^*$  values less than 0.4. Total number of analyses for each sample listed above plot, solid circles denotes average value for each plot, boxes extend from the 25<sup>th</sup> to the 75<sup>th</sup> quartile, middle line in the box defines the median, and the whiskers extend to the minimum and maximum values showing the full range of values. GLS = Gump Lake stock, min = mineralization.

samples (Fig. 4). This interpretation is supported by the fact that the dikes represent a very small source area compared to the rest of the intrusion and were, for the most part, covered during the last glaciation cycle and were not subjected to glacial erosion (Bobrowsky et al., 1993; Ferbey et al., 2016; Reman, 2019).

The  $\text{Eu}/\text{Eu}_N^*$  in Guichon Creek batholith zircons systematically increases from the older, more mafic marginal zones ( $\text{Eu}/\text{Eu}_N^* < 0.4$ ) to the younger felsic core zones, which host the copper deposits with mean  $\text{Eu}/\text{Eu}_N^*$  values  $> 0.5$  (Fig. 6b). Globally, magmatic zircon in porphyry copper deposits typically yields  $\text{Eu}/\text{Eu}_N^* > 0.4$ , related to the high water content and oxidation state of fertile intrusions (Ballard et al., 2002; Dilles et al., 2015; Shen et al., 2015; Lu et al., 2016, 2019;

Lee et al., 2017). The oxidized and hydrous nature of the core intrusive rocks ( $\text{Eu}/\text{Eu}_N^* > 0.4$ ) is detected in till zircon above and over 9 km down-ice from mineralization (Fig. 6a). Zircon from till samples located up-ice (DZ1), more than 12 km down-ice (DZ10 and DZ11), or in the marginal zone of the Guichon Creek batholith (DZ12) yielded mean  $\text{Eu}/\text{Eu}_N^*$  values  $< 0.4$  (Fig. 1), which is attributed to unmineralized or barren intrusions (Ballard et al., 2002; Lu et al., 2016). Based on these results, we suggest that the analysis of  $\text{Eu}/\text{Eu}_N^*$  in detrital zircon can be used as a regional discriminatory tool for fertility evaluation (Fig. 6). Additionally, fertility diagrams such as those shown in Figure 5 are based on extensive studies of porphyry copper deposits with significant discussion on their use as defining the oxidation state and fluid conditions of

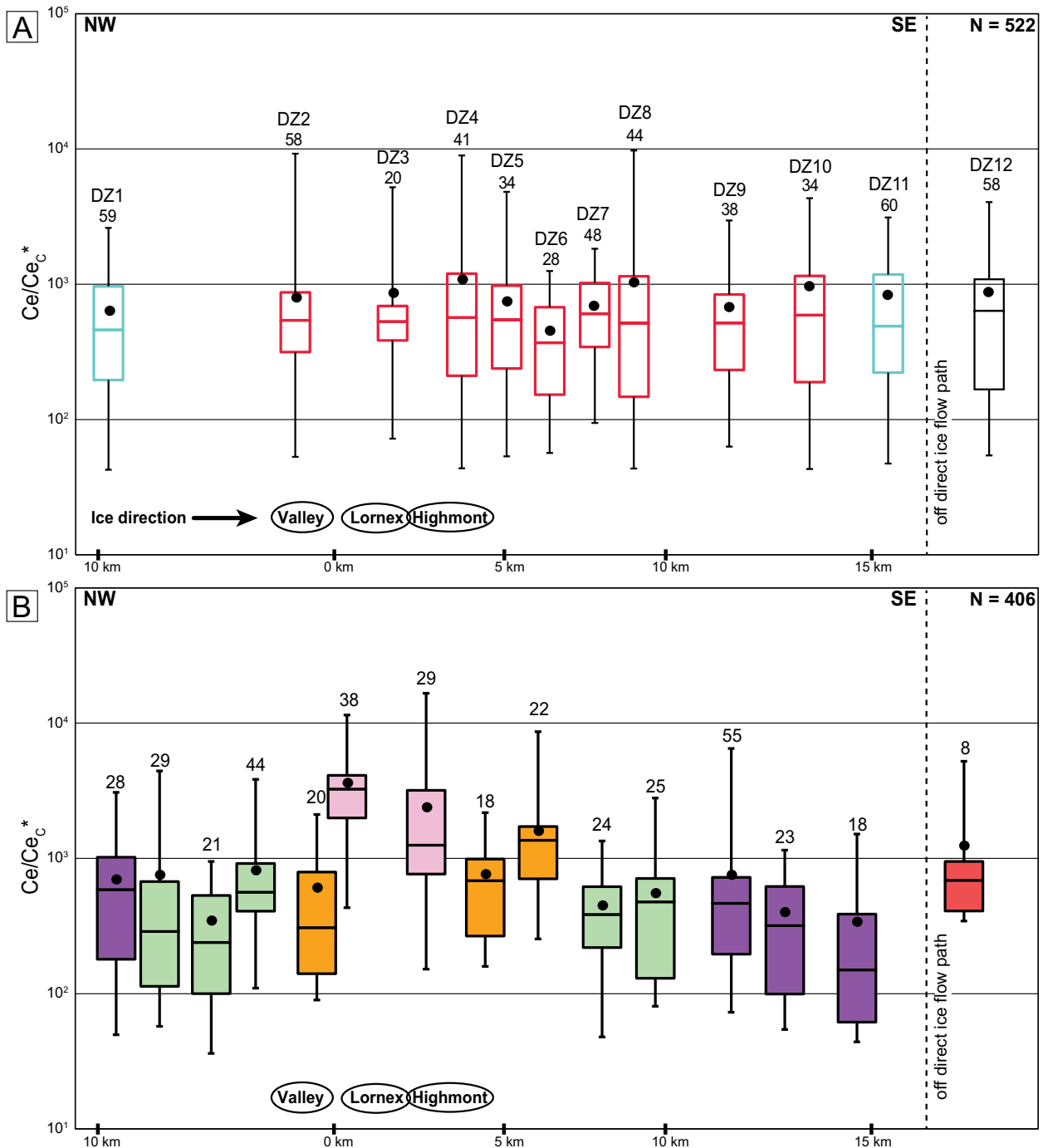


Fig. 7. Box and whisker plots of  $Ce/Ce_{c^*}$  zircon composition for A. Guichon Creek batholith detrital zircon samples and B. Guichon Creek batholith rocks. Format of the diagram same as in Figure 6.

the magma, with potential use in detecting porphyry copper deposits (Ballard et al., 2002; Dilles et al., 2015; Shen et al., 2015; Lu et al., 2016; Lee et al., 2017; Loader et al., 2017). Zircons from the till samples collected from the core of the batholith dominantly fall within the fields interpreted to be related to mineralization, relative to those zircons in the till samples collected distally from the main porphyry centers.

Contrary to  $Eu/Eu_{N^*}$ , the average  $Ce/Ce_{c^*}$  values in detrital till zircons do not record an anomalous signal over the

Guichon Creek batholith (Fig. 7a). In the Guichon Creek batholith intrusive phases,  $Ce/Ce_{c^*}$  ratios in zircon range from 35 to 16,500 across the margin to core samples (Fig. 7b), with the highest values ( $>1,000$ ) in the syn- to postmineral dikes and one of the core samples. The elevated  $Ce/Ce_{c^*}$  and elevated  $\Delta FMQ$  values (App. Fig. A1) in the late dikes are attributed to filter pressing from late magmatic crystallization yielding elevated Ce as well as Y, Nb, Ta, and REEs (Fig. 4) and reflect the late stage of the oxidation and fluid state



of the magma and not the main buildup to the mineralization potential of the magma, observed in the main igneous intrusions (Lee et al., 2020). In addition, the water content in the earlier intrusive phases of the Guichon Creek batholith could have contributed to the low  $Ce/Ce_C^*$  values in zircon from these phases (cf. Lu et al., 2019). Lastly, the small areal extent of the young stock and dikes (D'Angelo et al., 2017; Lee et al., 2020), which were partially to completely covered by preglacial sediments and volcanic rocks (McMillan, 1985; Bobrowsky et al., 1993), was not significantly eroded during glaciation, and therefore the young stocks and dikes contributed few zircons to the tills and were not captured by our samples. Consequently, the heterogeneously distributed  $Ce/Ce_C^*$  values in till zircon throughout the district are unrelated to the spatial relationship with mineralization but rather reflect the variability of  $Ce/Ce_C^*$  in magmatic rock zircons. While the calculated  $Ce/Ce_C^*$  and  $\Delta FMQ$  (App. Fig. A1) of the detrital zircon grains fall within error of the whole-rock values, there are no significant trends that can be correlated to mineralization potential. Further work may be merited to establish the potential use in detrital zircon to determine oxidation and fluid state of the source rock using zircon thermal and oxybarometer equations (Shen et al., 2015; Smythe and Brenan, 2015, 2016; Loucks et al., 2020).

Our case study of detrital zircon composition as a tool for mineral exploration in covered terrain shows that the  $Eu/Eu_N^* > 0.4$  that are typically observed in mineralized intrusions provide a regional signal detectable for over 9 km down-ice from mineralization in the Highland Valley Copper district (Fig. 1). This extended signal is due to the large exposures of the intrusive phases with  $Eu/Eu_N^*$  zircon values  $> 0.4$  and the resistant nature of zircon grains, which have survived glacial comminution and postglacial weathering. The zircon method presented here could be used in combination with other porphyry Cu indicator minerals such as sulfide, epidote, and apatite (Bouzari et al., 2016; Plouffe and Ferbey, 2017). In the search for porphyry mineralization not exposed to glacial erosion, i.e., present at depth in the intrusion or protected from glacial erosion by younger cover, zircon would be a useful tool to provide an indication of the intrusion fertility because some of these other indicator minerals directly linked to mineralization (e.g., chalcopyrite) would not be present in till. We suspect that the study of the composition of detrital zircons tested here in glaciated terrain would be equally applicable in an unglaciated terrain using other sample media (e.g., stream sediments).

In a study on zircon compositions conducted in the Late Triassic Granite Mountain batholith, host to the Gibraltar porphyry Cu-Mo deposit, 260 km northwest of the Highland Valley Copper district, only the Ce and not the Eu values in zircons provide an indication of fertility (Plouffe et al., 2019; Kobylinski et al., 2020). There, bedrock zircons from the mineralized intrusive phase (Mine phase) have an average  $Eu/Eu_N^* = 0.3$ , which is lower than the unmineralized phase (Granite Mountain phase;  $Eu/Eu_N^* = 0.5$ ) and the adjacent unmineralized Cretaceous Sheridan Creek stock (avg  $Eu/Eu_N^* = 0.6$ ; Kobylinski et al., 2018, 2020). On the other hand, zircon average  $Ce^{4+}/Ce^{+3}$  ratios are highest in the oldest mineralized Mine phase ( $Ce^{4+}/Ce^{+3} = 681$ ) compared to values in the unmineralized intrusive phases ( $Ce^{4+}/Ce^{+3}$

$\leq 212$ ; Kobylinski et al., 2018, 2020). In a study conducted by Wolfe (2017), 45 zircon grains from five till samples located  $< 10$  km up-ice and down-ice of the Gibraltar deposit were analyzed to investigate the potential for till zircon composition as an indicator of fertility. Using a threshold  $Ce^{4+}/Ce^{+3}$  value of 400, correlated to a Ce/Nd ratio of 20 (Kobylinski et al., 2018, 2020), only two zircon grains yielded a Ce/Nd ratio  $> 20$ , both from a single till sample located  $< 1$  km from mineralization (Plouffe et al., 2019). The  $Ce^{4+}/Ce^{+3}$  threshold of 400 at Gibraltar is high in comparison to a value of 300 defined by Ballard et al. (2002) in the Chuquicamata-El Abra porphyry copper belt in Chile, 120 used by Liang et al. (2006) at five ore-bearing porphyries and three barren ones in Tibet, and 120 also used by Shen et al. (2015) at nine porphyry Cu deposits of the Central Asian orogenic belt.

Apart from the oxidation state of an intrusion, other factors can influence the Eu and Ce anomalies in magmatic zircons. For instance, temperature (Smythe and Brenan, 2015, 2016) and water content of the melt (Lu et al., 2019) can affect Ce anomalies in magmatic zircon. CocrySTALLIZATION of other mineral phases such as titanite can impact zircon composition and could potentially create a false positive fertility signal with elevated Eu anomalies (Loader et al., 2017). This could account for the  $Eu/Eu_N^* > 0.4$  in the unmineralized intrusive phases at Gibraltar indicated above (Kobylinski et al., 2018). More studies that link REEs and oxybarometer (e.g., Loucks et al., 2020) in magmatic zircon with the fertility of an intrusion, along with the traceability of the anomalous signal in detrital zircon grains, need to be pursued to better constrain the efficiency and limitations of the zircon method as a widely applicable exploration tool.

Advances in LA-ICP-MS technology, which allows for the rapid acquisition of zircon composition (up to 500 grains/day), yielding both an age and a chemical characterization of the magma at the time of zircon crystallization, provide a strategic tool to identify a regional fertility signal associated to an intrusion. The number of analyses required to produce a statistical description of detrital zircon in a regional setting (Sircombe and Hazelton, 2004; Andersen, 2005) and the impact of the heavy mineral separation and picking procedures on the detrital zircon geochronology (Sláma and Košler, 2012) are topics of debate for detrital zircon studies applied to provenance analysis, correlation, and tectonic reconstructions. Our data suggest that within glaciated terrains, the analysis of detrital zircon grains recovered from 10 or more subglacial till samples, spatially distributed over several kilometers, reveals chemical differences that we correlate to a porphyry fertility magmatic signal. However, given the variability of zircon composition in a single intrusive phase and within a single till sample, analyses of multiple zircon grains are required. In our study, it was found that 14 to 31 zircon crystals per till sample are sufficient to define a broad regional pattern in  $Eu/Eu_N^*$  values that can be linked to the fertility potential of the Guichon Creek batholith.

## Conclusion

The REE compositions of till zircon grains can provide useful information on the mineralization potential of the underlying intrusion. In this case study conducted at the Highland Valley Copper district of south-central British Columbia,

the  $\text{Eu}/\text{Eu}_N^*$  ratios in till zircon grains indicate the fertility potential of the zircon source or host intrusion with average values  $>0.4$  for a distance of  $>9$  km down-ice from porphyry Cu mineralization. On the other hand, neither the  $\text{Ce}/\text{Ce}_c^*$  nor the  $\Delta\text{FMQ}$  of detrital zircons yielded an anomalous signal, because the intrusive phase with the highest zircon  $\text{Ce}/\text{Ce}_c^*$  and  $\Delta\text{FMQ}$  was not aerially extensive and was not fully exposed to glacial erosion to contribute sufficient anomalous zircon grains to the till matrix to be detected. Continued research on the composition of magmatic zircon in porphyry Cu systems along with the traceability of detrital zircon with a positive fertility signal will contribute toward the development of a widely applicable and effective mineral exploration method to detect buried porphyry systems. The presence of detrital zircon grain populations with average  $\text{Eu}/\text{Eu}_N^* >0.4$  provides an indication of elevated fluid and oxidation state in the source intrusion and higher potential for porphyry copper formation.

### Acknowledgments

Funding for this project was provided through the Natural Sciences and Engineering Research Council of Canada (NSERC) and the Canadian Mining Innovation Council (CMIC) Mineral Exploration Footprints project. The Geological Survey of Canada and the British Columbia Geological Survey provided support with funding from the Targeted Geoscience Initiative. Marghaleray Amini from the Pacific Centre for Isotopic and Geochemical Research (PCIGR) provided technical support for data collection. Teck Resources Limited is thanked for access to their Highland Valley Copper deposit and adjacent areas. This manuscript is NSERC-CMIC Mineral Exploration Footprints project contribution number 181, MDRU publication number 406, and Natural Resources Canada contribution number 20180190. An earlier version of this manuscript benefited from reviews by J.H. Dilles and N.M. Rayner. The authors would also like to thank Yongjun Lu for edits and comments on the manuscript.

### REFERENCES

- Ali, S.H., Giurco, D., Arndt, N., Nickless, E., Brown, G., Demetriades, A., Durrheim, R., Enriquez, M.A., Kinnaird, J., Littleboy, A., Meinert, L.D., Oberhänsli, R., Salem, J., Schodde, R., Schneider, G., Vidal, O., and Yakovleva, N., 2017, Mineral supply for sustainable development requires resource governance: *Nature*, v. 543, p. 367–372.
- Andersen, T., 2005, Detrital zircons as tracers of sedimentary provenance: Limiting conditions from statistics and numerical simulation: *Chemical Geology*, v. 216, p. 249–270.
- Ash, C.H., Reynolds, P.H., Creaser, R.A., and Mihalyuk, M.G., 2006,  $^{40}\text{Ar}/^{39}\text{Ar}$  and Re-Os isotopic ages for hydrothermal alteration and related mineralization at the Highland Valley Cu-Mo deposit (NTS 092I), southwestern British Columbia: British Columbia Geological Survey, Geological Fieldwork 2006, Paper 2007-1, p. 19–24.
- Averill, S.A., 2001, The application of heavy indicator mineralogy in mineral exploration with emphasis on base metal indicators in glaciated metamorphic and plutonic terrains: The Geological Society of London, Special Publication 185, p. 69–81.
- Ballard, J.R., Palin, J.M., and Campbell, I.H., 2002, Relative oxidation states of magmas inferred from  $\text{Ce(IV)}/\text{Ce(III)}$  in zircon: Application to porphyry copper deposits of northern Chile: *Contributions to Mineralogy and Petrology*, v. 144, p. 347–364, doi: 10.1007/s00410-002-0402-5.
- Belousova, E.A., Griffin, W.L., O'Reilly, S.Y., and Fisher, N.I., 2002, Igneous zircon: Trace element composition as an indicator of source rock type: *Contributions to Mineralogy and Petrology*, v. 143, p. 602–622.
- Bobrowsky, P.T., Kerr, D.E., and Sibbick, S.J., 1993, Drift exploration studies, Valley Copper pit, Highland Valley copper mine, British Columbia: Stratigraphy and sedimentology (92I/6, 7, 10 and 11): British Columbia Geological Survey, Geological Fieldwork 1992, Paper 1993-1, p. 427–437.
- Bouzari, F., Hart, C.J.R., Bissig, T., and Barker, S., 2016, Hydrothermal alteration revealed by apatite luminescence and chemistry: A potential indicator mineral for exploring covered porphyry copper deposits: *Economic Geology*, v. 111, p. 1397–1410, doi: 10.2113/econgeo.111.6.1397.
- Burnham, A.D., Berry, A.J., Halse, H.R., Schofield, P.F., Gibin, G., and Mosselmans, J.F.W., 2015, The oxidation state of Eu in silicate melts as a function of oxygen fugacity, composition and temperature: *Chemical Geology*, v. 411, p. 248–259.
- Byrne, K., Stock, E., Ryan, J., Johnson, C., Nisenson, J., Alva Jimenez, T., Lapointe, M., Stewart, H., Grubisa, G., and Syroka, S., 2013, Porphyry Cu-(Mo) deposits in the Highland Valley district, south-central British Columbia: Society of Economic Geologists, Field Trip Guidebook Series, v. 43, p. 99–116.
- Clague, J.J., and Ward, B.C., 2011, Pleistocene glaciation of British Columbia, in Ehlers, J., Gibbard, P.L., and Hughes, P.D., eds., *Developments in quaternary science*, v. 15: Amsterdam, Elsevier, p. 563–573, doi: 10.1016/B978-0-444-53447-7.00044-1.
- D'Angelo, M., Alfaro, M., Hollings, P., Byrne, K., Piercey, S., and Creaser, R.A., 2017, Petrogenesis and magmatic evolution the Guichon Creek batholith: Implications for the Highland Valley porphyry Cu  $\pm$  (Mo) district, south-central British Columbia: *Economic Geology*, v. 112, p. 1857–1888.
- Dilles, J.H., Kent, A.J.R., Wooden, J.L., Tosdal, R.M., Koleszar, A., Lee, R.G., and Farmer, L.P., 2015, Zircon compositional evidence for sulfur-degassing ore-forming arc magmas: *Economic Geology*, v. 110, p. 241–251, doi: 10.2113/econgeo.110.1.241.
- Elshkaki, A., Graedel, T.E., Ciacci, L., and Reck, B.K., 2016, Copper demand, supply, and associated energy use to 2050: *Global Environmental Change*, v. 39, p. 305–315.
- Ferbey, T., Plouffe, A., and Bustard, A.L., 2016, Geochemical, mineralogical, and textural data from tills in the Highland Valley Copper mine area, south-central British Columbia: British Columbia Geological Survey Geo-File 2016-11, Geological Survey of Canada Open File 8119, 1 zip file, doi: 10.4095/299242.
- Kelley, K.D., Eppinger, R.G., Lang, J., Smith, S.M., and Fey, D.L., 2011, Porphyry Cu indicator minerals in till as an exploration tool: Example from the giant Pebble porphyry Cu-Au-Mo deposit, Alaska, USA: *Geochemistry: Exploration, Environment, Analysis*, v. 11, p. 321–334, doi: 10.1144/1467-7873/10-IM-041.
- Kobylnski, C., Hattori, K., Smith, S., and Plouffe, A., 2020, Protracted magmatism and mineralized hydrothermal activity at the Gibraltar porphyry copper-molybdenum deposit, British Columbia: *Economic Geology*, v. 115, p. 1119–1136, doi: 10.5382/econgeo.4724.
- Kobylnski, C.H., Hattori, K., Smith, S.W., and Plouffe, A., 2018, High cerium anomalies in zircon from intrusions associated with porphyry copper mineralization in the Gibraltar deposit, south-central British Columbia: Geological Survey of Canada, Open File 8430, doi: 10.4095/311194.
- Lee, R.G., Dilles, J.H., Tosdal, R.M., Wooden, J.L., and Mazdab, F.K., 2017, Magmatic evolution of granodiorite intrusions at the El Salvador porphyry copper deposit, Chile, based on trace element composition and U/Pb age of zircons: *Economic Geology*, v. 112, p. 245–273.
- Lee, R.G., Byrne, K., D'Angelo, M., Hart, C.J.R., Hollings, P., Gleeson, S.A., and Alfaro, M., 2020, Using zircon trace element composition to assess porphyry copper potential of the Guichon Creek batholith and Highland Valley Copper deposit, south-central British Columbia: *Mineralium Deposita*, doi: 10.1007/s00126-020-00961-1.
- Liang, H.-Y., Campbell, I.H., Allen, C., Sun, W.-D., Liu, C.-Q., Yu, H.-X., Xie, Y.-W., and Zhang, Y.-Q., 2006, Zircon  $\text{Ce}^{4+}/\text{Ce}^{3+}$  ratios and ages for Yulong ore-bearing porphyries in eastern Tibet: *Mineralium Deposita*, v. 41, p. 152–159.
- Loader, M.A., Wilkinson, J.J., and Armstrong, R.N., 2017, The effect of titanite crystallisation on Eu and Ce anomalies in zircon and its implications for the assessment of porphyry Cu deposit fertility: *Earth and Planetary Science Letters*, v. 472, p. 107–119.
- Loucks, R.R., Fiorentini, M.L., and Henríquez, G.J., 2020, New magmatic oxybarometer using trace elements in zircon: *Journal of Petrology*, doi: 10.1093/ptrology/egaa034.
- Lu, Y., Smithies, R.H., Wingate, M.T.D., Evans, N.J., McCuaig, T.C., Champion, D.C., and Outhwaite, M., 2019, Zircon fingerprinting of magmatic-hydrothermal systems in the Archean Yilgarn craton: Geological Survey of Western Australia, Report 197, 22 p.

- Lu, Y.J., Loucks, R.R., Fiorentini, M., McCuaig, T.C., Evans, N.J., Yang, Z.-M., Hou, Z.-Q., Kirkland, C.L., Parra-Avila, L.A., and Kobussen, A., 2016, Zircon composition as a pathfinder for porphyry Cu  $\pm$  Mo  $\pm$  Au deposits: Society of Economic Geologists, Special Publication 19, p. 329–347.
- McMillan, W.J., 1985, Geology and ore deposits of the Highland Valley Camp: Geological Association of Canada, Mineral Deposits Division Field Guide and Reference Manual Series, no. 1, p. 1–121.
- McMillan, W.J., Anderson, R.G., Chan, R., and Chow, W., 2009, Geology and mineral occurrences (minfile), Guichon Creek batholith and Highland Valley porphyry copper district, British Columbia: Geological Survey of Canada, Open File 6079, scale 1:100,000 and 1:150,000, 2 sheets.
- Plouffe, A., and Ferbey, T., 2015, Surficial geology, Gnawed Mountain area, British Columbia, parts of NTS 921/6, I/7, I/10 and I/11: Geological Survey of Canada, Canadian Geoscience Map 214, British Columbia Geological Survey, Geoscience Map 2015-3, scale 1:50,000, doi: 10.4095/296285.
- 2017, Porphyry Cu indicator minerals in till: A method to discover buried mineralization: Mineral Association of Canada, Topics in Mineral Sciences, v. 47, Geological Association of Canada, Special Paper 50, p. 129–159.
- Plouffe, A., Ferbey, T., Hashmi, S., and Ward, B.C., 2016, Till geochemistry and mineralogy: Vectoring towards Cu porphyry deposits in British Columbia, Canada: Geochemistry: Exploration, Environment, Analysis, v. 16, p. 213–232, doi: 10.1144/geochem2015-398.
- Plouffe, A., Kjarsgaard, I.M., Kobylinski, C., Hattori, K., Petts, D.C., Venance, K.E., and Ferbey, T., 2019, Discovering the next generation of copper porphyry deposits using mineral markers: Geological Survey of Canada, Open File 8549, p. 321–331, doi: 10.4095/313666.
- Reman, A., 2019, Assessing stratigraphic controls on the secondary detrital footprint from buried mineralization and alteration at the Highland Valley Copper mine, British Columbia: Unpublished M.Sc. thesis, Ontario, Canada, University of Waterloo, 382 p.
- Schodde, R., 2017, Long term trends in global exploration: Are we finding enough metals?: Fennoscandian Exploration and Mining Conference, 11<sup>th</sup>, Levi, Lapland, Finland, October 31–November 2, Technical Program.
- Shen, P., Hattori, K., Pan, H., Jackson, S., and Seitmuratova, E., 2015, Oxidation condition and metal fertility of granitic magmas: Zircon trace-element data from porphyry Cu deposits in the Central Asian orogenic belt: Economic Geology, v. 110, p. 1861–1878.
- Shu, Q., Chang, Z., Lai, Y., Hu, X., Wu, H., Zhang, Y., Wang, P., Zhai, D., and Zhang, C., 2019, Zircon trace elements and magma fertility: Insights from porphyry (-skarn) Mo deposits in NE China: Mineralium Deposita v. 54, p. 645–656, doi: 10.1007/s00126-019-00867-7.
- Sircombe, K.N., and Hazelton, M.L., 2004, Comparison of detrital zircon age distributions by kernel functional estimation: Sedimentary Geology, v. 171, p. 91–111.
- Sláma, J., and Košler, J., 2012, Effects of sampling and mineral separation on accuracy of detrital zircon studies: Geochemistry Geophysics Geosystems, v. 13, 17 p.
- Smythe, D.J., and Brenan, J.M., 2015, Cerium oxidation state in silicate melts: Combined  $f_{O_2}$ , temperature and compositional effects: *Geochimica et Cosmochimica Acta*, v. 170, p. 173–187, doi: 10.1016/j.gca.2015.07.016.
- 2016, Magmatic oxygen fugacity estimated using zircon-melt partitioning of cerium: *Earth and Planetary Science Letters*, v. 453, p. 260–266, doi: 10.1016/j.epsl.2016.08.013.
- Sverdrup, H.U., Olafsdottir, A.H., and Ragnarsdottir, K.V., 2019, On the long-term sustainability of copper, zinc and lead supply, using a system dynamics model: *Resources, Conservation and Recycling: X*, v. 4, article 100007, doi: 10.1016/j.rcrx.2019.100007.
- Teck Resources Limited, 2019, Annual report: [www.teck.com/media/2019-Annual-Report.pdf](http://www.teck.com/media/2019-Annual-Report.pdf), accessed February 2020.
- Whalen, J.B., Davis, W.J., and Anderson, R.A., 2017, Temporal and geochemical evolution of the Guichon Creek batholith and Highland Valley porphyry copper district, British Columbia: Implications for generation and tectonic setting of porphyry systems: Geological Survey of Canada, Open File 8334, doi: 10.4095/306147.
- Wolfe, L., 2017, Chemistry of refractory indicator minerals in tills around the Gibraltar porphyry copper deposit, southcentral British Columbia: Unpublished B.Sc. thesis, Ottawa, Canada, University of Ottawa, 56 p.
- Zhong, S., Seltmann, R., Qu, H., and Song, Y., 2019, Characterization of the zircon Ce anomaly for estimation of oxidation state of magmas: A revised Ce/Ce<sup>o</sup> method: *Mineralogy and Petrology*, v. 113, p. 755–763, doi: 10.1007/s00710-019-00682-y.



**Robert G. Lee** is a porphyry copper geologist with extensive industry experience and has responsibility for Mineral Deposit Research Unit (MDRU) geochronological and isotopic projects at the University of British Columbia, Canada. He holds an M.Sc. degree from Washington State University (2004) and a Ph.D. degree from Oregon State University (2008). Before joining MDRU, he spent eight years working on greenfield and brownfield projects with Freeport McMoran Copper and Gold Inc. Robert was previously a lead research associate in the Natural Sciences and Engineering Research Council of Canada (NSERC) and the Canadian Mining Innovation Council (CMIC) Mineral Exploration Footprints project, where he oversaw the logistics and all research at the Teck Resources Limited Highland Valley Copper deposit in south-central British Columbia.

